atmosphere

MDPI

Article

Future Changes in Thermal Bioclimate Conditions over West Bengal, India, Based on a Climate Model

Sourabh Bal [1,2,*] and Ingo Kirchner [2]

[1] Department of Physics, Swami Vivekananda Institute of Science & Technology, Kolkata 700145, India
[2] Institute for Meteorology, Freie Universität, 12165 Berlin, Germany
* Correspondence: sourabhbal@gmail.com or sourabhbal@zedat.fu-berlin.de

Abstract: Changes in extreme human bioclimate conditions are accepted evidence for and serve as a broad measure of anthropogenic climate change. The essential objective of the current study was to investigate past and future thermal bioclimate conditions across West Bengal (WB), India. The daily physiologically equivalent temperature (PET) was calculated by considering definite climate variables as inputs. These meteorological variables were captured from the Coordinated Regional Downscaling Experiment (CORDEX)-South Asia. The initial results from this research work present the mean monthly distribution of each PET class over the considered stations of WB during the period (1986–2005) and three future time periods: (i) near future (2016–2035), (ii) mid-future (2046–2065), and (iii) far future (2080–2099). It was observed that the months from April to June comprise heat stress months in terms of human thermal perception, whereas thermally acceptable conditions begin in November and continue until March for most stations. Results from future PET changes over WB in the context of the reference period (1986–2005) reveal a prominent increase in warm and hot PETs for all future time periods in two different greenhouse gas emission scenarios. During the far-future time period, stations within a kilometer of the Bay of Bengal such as Digha, Diamond Harbour, Canning, and Baruipur account for the highest percentage in the warm PET class (35.7–43.8 °C) in high-end emission scenarios. Simultaneously, during the period from 2080 to 2099, Kolkata, Dum Dum, Kharagpur, and Siliguri will experience a PET greater than 43.8 °C for close to 10% of the days in the year and more than 10% in Sriniketan, Malda, Asansol, and Birbhum. During the far-future period, a negative change in the very cool PET class (<3.3 °C) indicating a decrease in cold days was the largest for Darjeeling.

Keywords: West Bengal; physiologically equivalent temperature (PET); RayMan model; climate model; CORDEX-South Asia

Citation: Bal, S.; Kirchner, I. Future Changes in Thermal Bioclimate Conditions over West Bengal, India, Based on a Climate Model. *Atmosphere* **2023**, *14*, 505. https://doi.org/10.3390/atmos14030505

Academic Editor: Tanja Cegnar

Received: 22 October 2022
Revised: 19 February 2023
Accepted: 21 February 2023
Published: 5 March 2023

1. Introduction

According to the Intergovernmental Panel on Climate Change (IPCC) report and the prediction from climate models, there will be an increase in global air temperature in the future [1–4]. The variation in the mean air temperature may cause a rise in extreme temperatures [5,6]. Similarly, changes in the trends and patterns of other climate variables along with extreme air temperatures have a cumulative impact on human health, agriculture, and national economies [7,8]. Recent studies report that extreme heat episodes are increasing across almost all land regions across the globe [9–13]. India has also shown significant warming trends in tune with the global warming pattern [14–17]. Studies related to the heat wave in India based on the daily maximum temperature identified a few stations from north, northwest, and central India with a significant increase in heat wave trends [18–21]. West Bengal (WB), a state from eastern India, stretches from the Himalayas in the north to the Bay of Bengal in the south and is protected by the progressive delta of the Sundarbans mangrove forest. There are many states in India, including Gangetic WB, that register heat wave spells for 8 days on average [22–24]. Every year, hundreds of citizens are admitted

to hospitals due to heat-related illnesses in India [25]. Rapid changes in temperature may also alter the balance between humans and parasites and thereby increase the chances of mosquito-borne diseases such as malaria and dengue [26]. Human thermal perception comprises the capacity to accommodate the body temperature within certain limits. If the human body confronts a situation beyond these limits, the thermoregulation system tries to balance out the additional heat gain or heat loss. Under extreme thermal conditions, the thermoregulation system breaks down with changes in the body's core temperature (37 °C) and causes human thermal stress that may lead to human thermal discomforts such as muscle cramps, exhaustion, and life-threatening heat strokes [27–30].

Human bioclimate conditions could be estimated with air temperature, relative humidity, wind speed, and mean radiant temperature. Furthermore, cloud cover plays an important role in computing the mean radiant temperature [31–35]. Several studies reported that personal parameters on a personal level such as age, gender, clothing, and activity levels influence human thermal stress [36,37]. Human thermal perception should be estimated by complex models due to food and beverage intake and clothing insulation [38–40].

In recent years, multiple human bio-meteorological indices were recognized based on human heat budget models to categorize and scale human thermal stress. Some well-documented bioclimate indices are physiologically equivalent temperature (PET) [30,41,42], perceived temperature (PT) [29,43], standard effective temperature (SET) [28,44], and the recently developed Universal Thermal Climate Index (UTCI) [33,35]. These indices improve the cumulative effects of all thermal, physical, and physiological parameters to advance the evaluation of ambient conditions [34]. PET has been extensively used and categorized for the estimation of human bio-meteorological conditions and other aspects, such as worldwide tourism [45–47]. Amongst these indices, PET and UTCI have been broadly employed in recent studies due to their simple, sophisticated, and economical approach. The PET, in particular, proved efficient in different climate zones [48], and also against UTCI, its value can be estimated at zero wind speeds.

Due to the close association between the thermoregulatory system of the human body and weather, climate change modifies the number of heat stress days in most land areas of the world [49]. In the past decade, heat waves caused more deaths compared to other natural disasters in India, and in the year 2022, heat waves were responsible for at least 90 deaths across India and Pakistan [50]. A recent study reported that a few coastal subtropical locations experienced extremely humid heat episodes, and in terms of frequency, they have doubled in the last four decades [51]. Most of the research work conducted on bioclimatic environments over WB is limited for a short time period [52–56]. However, research studies focused on the validation of long-term trends of regional human thermal stress over WB are scarce. The maximum (in May) and minimum (in December and January) values of the mean monthly PET were reported by Bhattacharya, Biswas [57] for Kolkata and by Jaswal, Padmakumari [20] for the Indian subcontinent. The presence of hot stress days at the end of the twentieth century and the beginning of the twenty-first century was noted in urban stations. However, the observed station data of Diamond Harbour from 2018 to 2020, situated a few hundred kilometers from Kolkata, confirmed heat stress conditions. This impression of stations close to the Bay of Bengal being exposed to enhanced heat stress has also been observed by Jaswal, Padmakumari [20] and Rao, Kumar [58]. The former study identified the Indo Gangetic plain during monsoons as vulnerable to conditions inducing human thermal discomfort [20]. A recent study also projected heat stress over India under different emission scenarios and reported that the east coast region suffers more heat stress days than the western coastal regions [58].

Therefore, this present research concentrates on the human bio-meteorological environment in WB, which is reproduced from the climate model during past and future time scales. Furthermore, the spatial extent of human thermal comfort in terms of PET across 15 different stations of WB under different carbon dioxide emission concentration pathway scenarios is presented. The results will potentially advise local administrators in mak-

ing policies for improving human health, urban design, planning, population migration, tourism development, social culture, and economy.

2. Study Regions

WB is situated in the eastern part of India (20°31′–27°12′ N and 85°50′–89°52′ E) and comprises an area of approximately 88,752 sq. km (Figure 1). It is the second most densely populated state in India, with a population of more than 80 million people. In the North, it is bordered by the Himalayan Mountains. To the west lies the Chhotanagpur plateau, and the Southeast region comprises the plains of the Ganga–Brahmaputra delta, which culminates in the Bay of Bengal. The state shares international borders with Bangladesh in the east, Bhutan in the north, and Nepal in the northwest. Within India, WB shares its borders with the states of Bihar in the west, Orissa in south, Sikkim in the north, and Assam in the northeast.

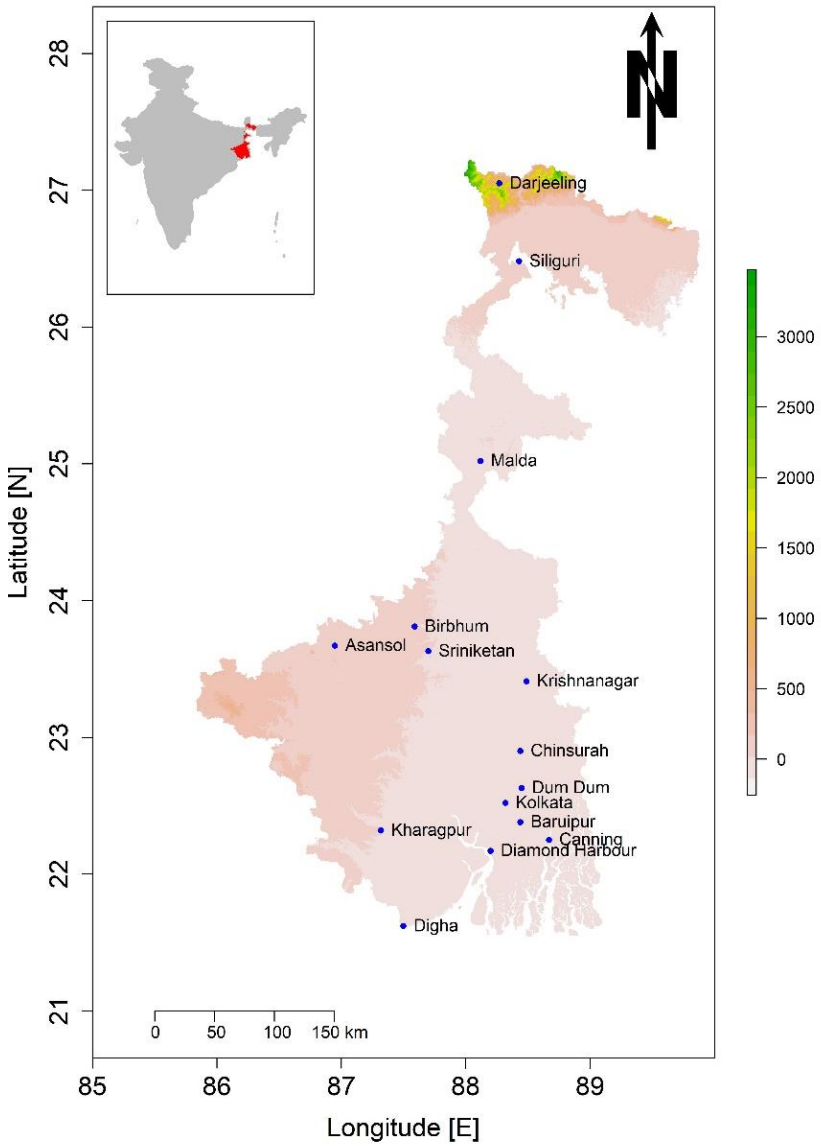

Figure 1. The considered 15 investigated sites are inscribed on the orography map of WB (WB). Inset: the political map of India. WB is highlighted (red) in the India map.

Based on Koppen's classification, the climate pattern of WB is classified into one of three types. The major parts of the Sub-Himalayan WB experiences sub-tropical monsoons and mild and dry winters, followed by hot summers (Cwa). The Gangetic WB and neigh-

boring southern parts of the Sub-Himalayan WB belong to the following type: hot tropical savanna, with seasonally dry winters (Aw). However, with respect to the northern-most parts of the Sub-Himalayan WB, viz., Darjeeling observed a tropical upland climate characterized by mild and dry winters and short summers (Cwb). The stations included in the Gangetic WB region for this study include Digha, Diamond Harbour, Canning, Baruipur, Alipore (Kolkata), Dum Dum, Kharagpur, Chinsurah, Krishnanagar, Sriniketan, Asansol, and Birbhum. The stations included for the Sub-Himalayan WB include Malda in the south and Darjeeling and Siliguri in the north [59].

WB's climate can be classified into four major seasons: winter: (December to February); summer: (March to May); southwest monsoon: (June to September); retreating southwest monsoon: (October to November). During the summer season, the daily temperature varies between 24 °C and 40 °C. During winter, the temperature varies from 7 °C to 26 °C. A few western districts in WB endure frequent heat waves in the summer months when the maximum temperature rises to 45 °C or above, whereas northern hilly districts experience infrequent snowfall when the minimum temperature reaches sub-zero.

May and April are the hottest months in the Gangetic and Sub-Himalayan WBs, with mean maximum temperatures of 35.6 °C and 33.8 °C, respectively. January is the coldest month in the state when the mean minimum temperatures for the Gangetic WB and Sub-Himalayan WB are 13.3 °C and 10.5 °C, respectively. The relative humidity is generally high during the period from July to September. The morning humidity levels reach 80% in June, which then rises to about 83–85% in July, August, and September. The period from December to March has sparse cloud cover. During the monsoon season from June to September, the skies are heavily clouded, particularly during July and August, when approximately 6 oktas of the sky is covered with clouds. Beginning in October, the cloud cover in the state decreases to a great extent [59,60].

The total annual recorded rainfall increases from 142 cm over the southern plains of WB to 371 cm over the northern parts while it decreases to 116 cm over the northwestern parts of Gangetic WB. The amount of rainfall varies significantly in the foothills of the Himalayas (205 cm to 405 cm). The southwest monsoon sets in over the state around the first week of June and covers the entire state by the second week of June. July is the rainiest month in the Sub-Himalayan WB and Gangetic WB. The Southwest Monsoon is the primary rainy season when the plains of WB receive 74–83% of the annual rainfall amount while the hills of WB receive 73–87%. Rainfall in the winter season accounts for approximately 3% of the annual total rainfall in Gangetic WB and 5% for the hills of WB. The withdrawal of the southwest monsoon begins from the northern parts of the state towards the end of the first week of October, and by the second week, the monsoon withdraws from the entire state [59]. The descriptive statistics for temperature, relative humidity, wind speed, and cloud cover for the 15 different locations across WB that were considered for the present study are presented in the Supplementary Tables.

3. Data

The long-term characteristics of anthropogenic thermal stress in WB have been inspected in the past using PET. This was performed by using the daily mean values of air temperature (°C), relative humidity (%), wind speed (ms^{-1}), and cloud cover (octas). To estimate the daily human thermal stress, PET changes were estimated for the period from 1986 to 2005 for all the selected sites and by using the daily meteorological variables obtained from the suite of the Coordinated Regional Downscaling Experiment (CORDEX) [61]. The future evolution of PET under the two representative concentration pathways (RCPs), RCP4.5 and RCP8.5, were also extracted from CORDEX. The two RCPs detail the feasible limits of the radiative forcing of greenhouse gases in the twenty-first century, with a +4.5 and +8.5 W per sq m, respectively. The CORDEX project consists of 13 unique domains. The present study used the South Asian domain of CORDEX. The South Asian domain consists of the geographical areas falling under the coordinates of 19.25° E–116.25° E and 15.75° S–45.75° N. The CORDEX models have a 0.44-degree arc spatial resolution,

which allows for a better account of topographic details, thereby producing quality outputs for the atmospheric variables of the near-surface temperature (K), surface relative humidity (%), total cloud cover (%), and near-surface wind speed (ms^{-1}). The time series of each variable for a given station was reproduced after selecting the nearest grid that corresponded to the coordinates defined in Table 1. Global climate models are used for wide-scale spatial analysis in the long-term projection of climate trends. However, they lack detailed information for local levels, which need to be fed into the model. With regard to the current study, the data quality of CORDEX for the entire domain of WB is comparable to the Era-Interim reanalysis for the period from 1979 to 2005 (illustrated in Figure 2). The boxplot (Figure 2) represents the descriptive statistics of temperature, relative humidity, cloud cover, wind speed, and PET between CORDEX and Era-Interim. It can be observed that the comparison clearly exhibits a good agreement for all variables between the two datasets. Hence, the mean PET values estimated from imported meteorological variables exhibit a difference of 1.8 °C between CORDEX and Era-Interim. A recent study investigated the PET variation for a few sites in WB at 1130 h and 1730 h by using the Era-Interim and Indian Meteorological Department datasets and confirmed the concurrence between the datasets (Bal and Matzarakis [60]). Therefore, removing the bias from CORDEX datasets could allow the classification of PET under the same thermal comfort category. Furthermore, the highest correlation coefficient value was observed to be 0.9 for temperature, 0.6 for relative humidity, 0.4 for cloud cover, and 0.3 for wind speed. Several studies on the impact of climate change on human bioclimate conditions have been performed on different geographical areas by using the output from a wide spectrum of regional climate models. CORDEX-East Asia and EURO-CORDEX have been successfully implemented in China and Europe, respectively, for studying the human bio-meteorological environment [62,63].

Table 1. List of the 15 selected stations with position coordinates along with their altitudes in WB for this study.

Sl. No.	Station	Abbreviated Station Code	Longitude	Latitude	Altitude (m)
1.	Digha	DGH	87.50° E	21.62° N	6
2.	Diamond Harbour	DHR	88.20° E	22.17° N	4
3.	Canning	CAN	88.67° E	22.25° N	4
4.	Baruipur	BRP	88.44° E	22.38° N	9
5.	Alipore (Kolkata)	KOL	88.32° E	22.52° N	6
6.	Dum Dum	DMM	88.45° E	22.63° N	6
7.	Kharagpur	KGP	87.32° E	22.32° N	61
8.	Chinsurah	CNH	88.44° E	22.90° N	200
9.	Krishnanagar	KNG	88.49° E	23.41° N	14
10.	Sriniketan	SRN	87.70 ° E	23.63° N	59
11.	Asansol	ASN	86.95° E	23.67° N	111
12.	Birbhum	BRM	87.59° E	23.81° N	71
13.	Malda	MLD	88.12° E	25.02° N	31
14.	Siliguri	SGR	88.43° E	26.48° N	122
15.	Darjeeling	DRJ	88.27° E	27.05° N	2128

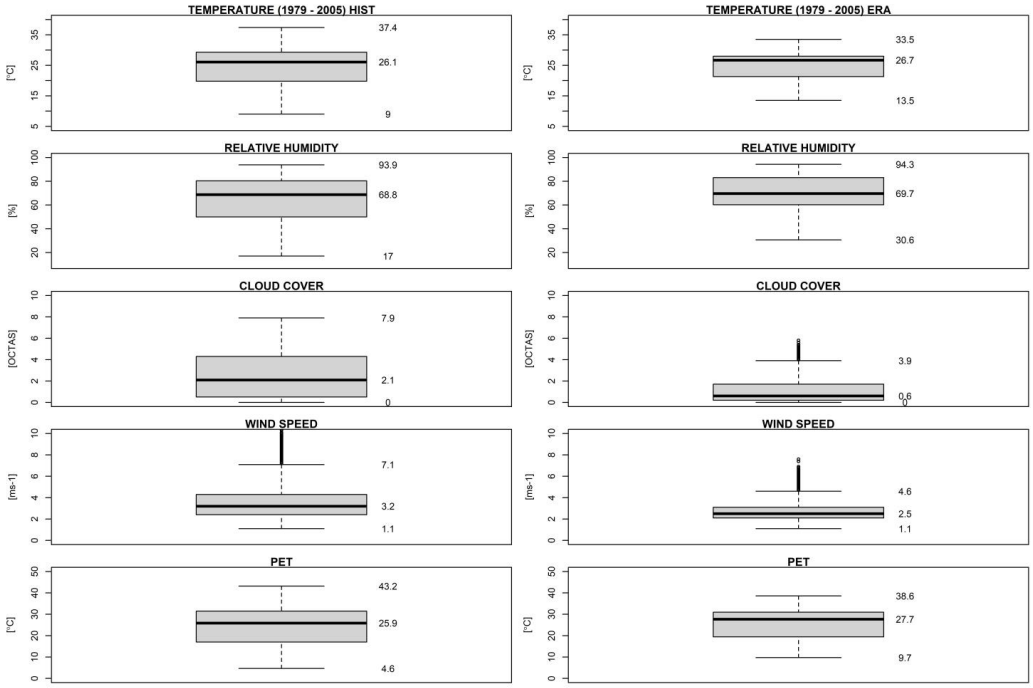

Figure 2. Represents the descriptive statistics of daily temperature, daily relative humidity, daily cloudy cover, daily wind speed, and daily PET extracted from Era-Interim (ERA) and CORDEX (HIST) over WB during the period from 1979 to 2005.

4. Applied Methodology

In this study, select atmospheric variables of air temperature, relative humidity, wind speed, and cloud cover were used to compute the PET in 15 stations across WB for different time periods by using RayMan Pro Model Version 3.1 [64,65]. PET is based on the Munich Energy-Balance Model for Individuals (MEMI), a two-node thermo-physiological heat-balance model. It is defined as the air temperature at which, in reference to an environment's setting, balancing occurs between the heat budget of the human body and the skin temp under complex outdoor conditions [66]. This model is also endorsed by German VDI Guideline 3787, Part 2. In the present study, the mean radiant temperature was estimated from cloud cover data due to the non-availability of solar radiation station data as an input variable in the RayMan model [40,67]. This approach of calculating the mean radiant temperature from cloud cover has been successfully reported in a past study [68]. Furthermore, the physiological aspects of the human body, such as clothing, gender, and age, play an important role in estimating PET [42]. Personal data such as height, weight, age, and sex were pre-determined as 1.75 m, 75 kg, 35 years, and male, respectively. The variables of clothing, activity, and position were pre-determined as 0.60, 80, and standing, respectively. A past study noted that slight changes in personal data did not modify the PET values when considering larger scales [55]. Keeping the personal data intact for each simulation, the daily PET was obtained for all 15 stations for the period of 1986–2005 and the future period of 2016–2099. The data are highlighted in Table 1. The PET class limit that is considered to be significant is characterized, especially for regional or local studies. In the initial stages of fixing the neutral temperature of PET, its ranges were delineated based on the European climate. Researchers had to modify the PET classes in different climatic regions. For example, the neutral PET range for the hot arid climate in Cairo, Egypt, was noted to be between 24.3 and 29.5 °C [69], while for the Mediterranean climate in Crete, Greece, the PET's neutral temperature limit was 20–25 °C [70]. Another study conducted for the city of Dhaka, which possesses a hot and humid tropical climate, reproduced PET ranges based on the hypothesis of Lin and Matzarakis [71]. The aforementioned studies adjusted the PET ranges using a two-step process. In the first step, the mean thermal sensation vote for

each 1 °C was calculated, followed by fixing the thermally acceptable range corresponding to the mean thermal sensation vote in step two. Several recent studies have adapted this method to update the temperature limit of each thermal class for several indices in different climatic zones. In recent studies focussing on India, modified PET ranges have been noted. This study also adopted a recent study's corrected PET classification, which was adjusted for Kolkata [52], the data for which are presented in Table 2. To capture the relative changes in future PET and its classes under different emissions conditions for all 15 sites in WB, three future periods were considered with respect to the past period (1986–2005). The three future periods were (i) near future (2016–2035), (ii) mid-future (2046–2065), and (iii) far future (2080–2099). The present study aimed to investigate the changes in PET for a time span of 20 years based on the methodology of a past study [58]. Additionally, the mean monthly PET differences for all three future periods in the context of the past years are presented under RCP4.5 and RCP8. The relative changes in each PET class and the mean monthly PET differences [52] are expressed as $(\Delta PET)_{class}$ and (ΔPET), respectively, for all three future time periods. As the temperature has significant weightage in deciding bioclimatic indices, the difference in mean monthly temperature (ΔTemp) for any station was compared to the difference in mean monthly PET for all three future time periods under RCP4.5 and RCP8.5. The changes in PET and Temperature are expressed as follows:

$$\Delta\mathbf{PET_{class}} = \mathbf{PET_{class,\ STN,PERIOD}} - \mathbf{PET_{class,STN,REFERENCE}} \quad (1)$$

$$\Delta\mathbf{PET} = \mathbf{PET_{STN,PERIOD}} - \mathbf{PET_{STN,REFERENCE}} \quad (2)$$

$$\Delta\mathbf{Temp} = \mathbf{Temperature_{STN,PERIOD}} - \mathbf{Temperature_{STN,REFERENCE}} \quad (3)$$

- **class** = Cold, Cool, Slightly cool, Neutral, Slightly warm, Warm, Hot;
- **STN** = Digha, Diamond Harbour, Canning, Baruipur, Alipore (Kolkata), Dum Dum, Kharagpur, Chinsurah, Krishnanagar, Sriniketan, Asansol, Birbhum, Malda, Siliguri, Darjeeling;
- **PERIOD** = 2016–2035, 2046–2065, 2080–2099;
- **REFERENCE** = 1986–2005.

Table 2. Categorized PET equivalent temperatures as a function of the thermal sensation for Kolkata [52], Taiwan [71], Western European cities [72–74], and Dhaka [75]. This present study used the PET classification of Kolkata [52].

Thermal Sensation	PET Range for Western European Cities (°C)	PET Range for Taiwan (°C)	PET Range for Dhaka (°C)	PET Range for Kolkata (°C)
Very cold	<4	<14		
Very cool/Cold	4–8	14–18		<3.31
Cool	8–13	18–22	23.5–26.5	3.31–11.42
Slightly cool	13–18	22–26	26.5–29.5	11.42–19.48
Neutral	18–23	26–30	29.5–32.5	19.48–27.59
Slightly warm	23–29	30–34	32.5–35.5	27.59–35.73
Warm	29–35	34–38	35.5–38.5	35.73–43.83
Hot	35–41	38–42	>38.5	>43.83
Very Hot	>41	>42		

5. Results

5.1. Monthly Variation of PET

The monthly frequency spectrum of PET for all the considered stations in WB during the historical period (1986–2005) depicts various PET classes starting from very cool to hot

conditions (as illustrated in Figure 3). Heat stress conditions in terms of slightly warm, warm, and hot classes together registered a minimum share of 80% during the period from April to August in all stations, except in Krishnanagar, Chinsurah, and Darjeeling. The 80% share of the minimum heat stress remained intact for two or more months, i.e., July and August, except for the stations of Chinsurah and Krishnanagar. Darjeeling is situated a few thousand meters above the mean sea level; therefore, the monthly PET distribution exhibited acceptable human thermal conditions for the period from March to September. Extreme heat stress conditions, designated as the hot class with a PET value of more than 43.83 °C, were observed in June with the following percentage shares: Sriniketan (8%), Kharagpur (6.8%), Birbhum (8.2%), Asansol (6.5%), Kolkata (3.2%), and Dum Dum (3.5%). In the near-future time period (2016–2035), under the RCP4.5 scenario (Supplementary Figure S1, left graph), the percentage share of hot conditions (>43.8 °C) in June decreased in a few urban stations, which was indicative of decreased anthropogenic forcings. In the near future, in the RCP8.5 scenario (Supplementary Figure S1, right graph), the number of days with a hot PET class increases slightly in comparison to the RCP4.5 scenario for all noted hot condition stations. The aforementioned changes were noted to increase further towards the end of the 21st century (Supplementary Figure S2). In the far future (2080–2099), under the RCP4.5 scenario (Supplementary Figure S3, left graph), the percentage share of hot stress conditions was (>43.83 °C) 7.2 % in May and 12% in June for Kolkata; 7.4% in May and 13.3% in June for Dum Dum; 12.4% in May and 17.2% in June for Kharagpur; 20.3% in May and 23.6% in June for Sriniketan; 20.8% in May and 22.3% in June for Asansol; 21.1% in May and 23.3% in June for Birbhum; 9.3% in May and 16.2% in June for Malda; and 9.8% in June and 7.4% in July for Siliguri, respectively. In the higher emission scenario, the aforementioned stations could potentially experience a two-to-three-fold increase in hot stress conditions (Supplementary Figures S4–S6).

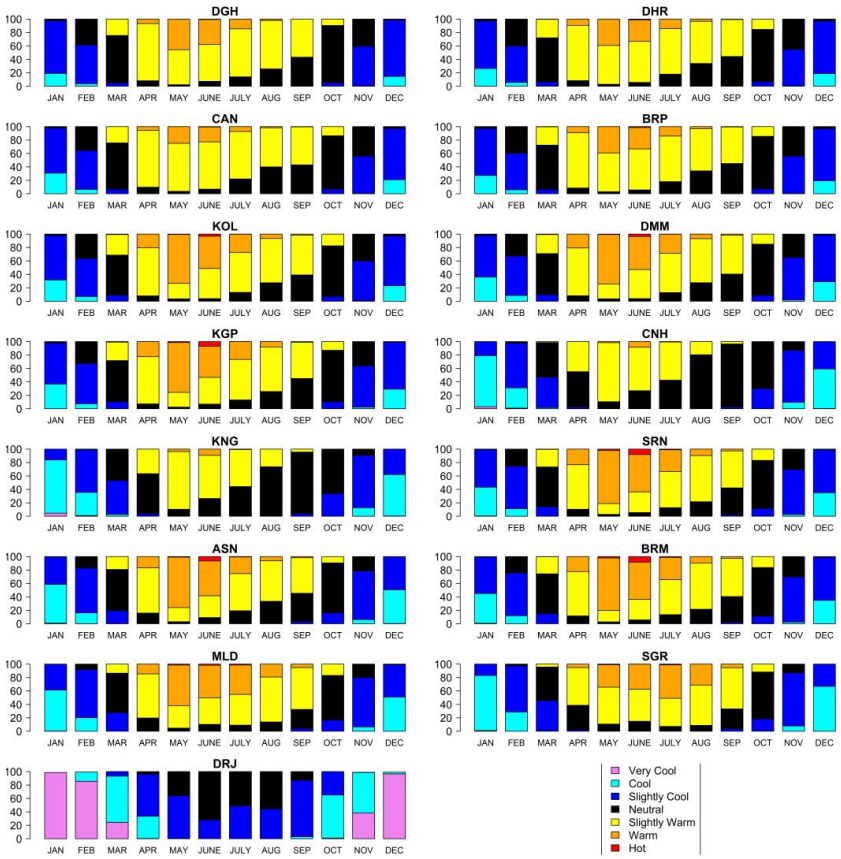

Figure 3. Intra-annual PET distribution of each category over the investigated stations extracted from the historical simulation of CORDEX (1986–2005). The abbreviations of each station are explained in Table 1.

5.2. Future Changes in PET against the Past Period under Different RCP Scenarios

The results obtained in this study accounted for the spatial variability of the monthly biothermal conditions in WB. The current study also evaluated the future changes in PET classes (in %) relative to the reference period of 1986–2005. Three future time periods of (i) near future (2016 to 2035), (ii) mid-future (2046 to 2065), and (iii) far future (2080 to 2099) were considered with respect to two emission scenarios. Figure 4 illustrates the changes in the three different future periods' PET values for the fifteen stations investigated under the RCP4.5 and RCP8.5 scenarios. The overall relative PET classes highlighted that in the time period from near future to far future, thermal stress conditions comprised slight warm, warm, and hot, with all three conditions exhibiting a significant increase except for Darjeeling. The maximum decrease in the very cool stress values calculated for Darjeeling towards the end of this century was 22%. Consequently, the magnitude of the percentage change was found to increase during the transition from near future to far future relative to the reference period. Even the percentage change in thermal stress conditions was found to be higher in the RCP8.5 scenario compared to the RCP4.5 scenario for each future time period. During the far future time period under the RCP8.5 scenario, Sriniketan, Asansol, Birbhum, and Malda could potentially experience prominent hot conditions of 10–12.5%. Hot conditions could potentially occur in the urban stations of Kolkata, Dum Dum, Kharagpur, and Siliguri (6.2–8.8%). Stations such as Digha, Diamond Harbour, Canning, and Baruipur, which are close to the Bay of Bengal, would potentially experience the most unpleasant warm thermal conditions. Hot conditions were not observed in the far future for the stations of Darjeeling, Chinsurah, and Krishnanagar. The largest decrease in any thermal condition was observed in Darjeeling with regard to very cool stress conditions under the RCP8.5 scenario, especially during the last decade of the century.

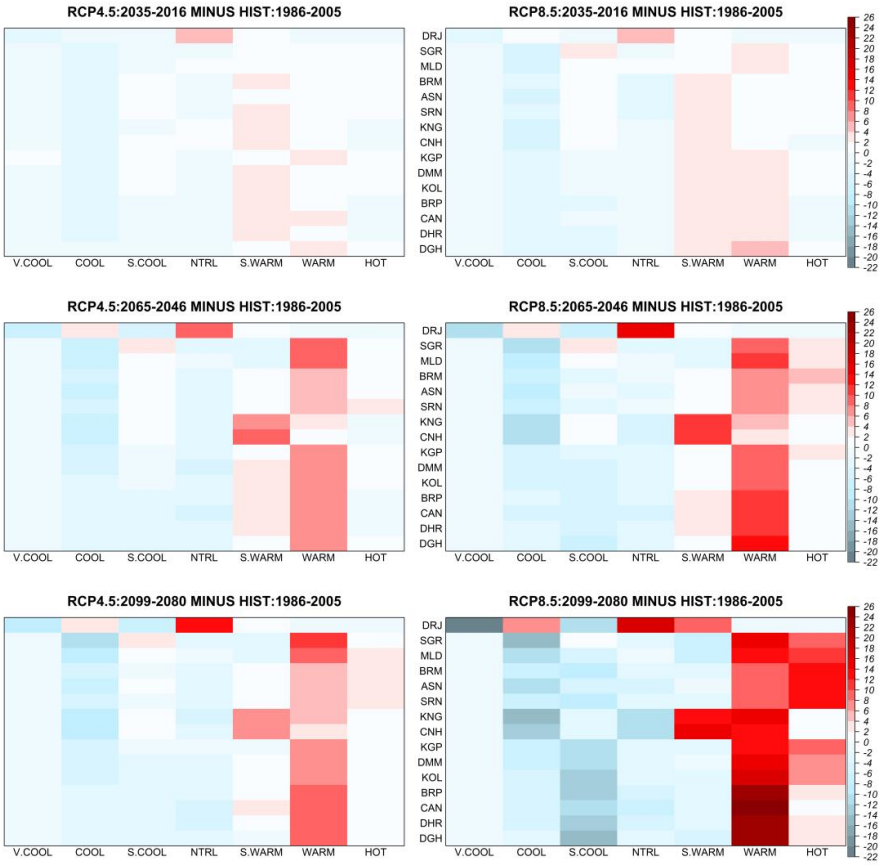

Figure 4. Relative variation of PET thermal stress categories (%) at 15 considered stations in WB under RCP4.5 and RCP8.5 from CORDEX during (i) 2016–2035, (ii) 2046–2065, and (iii) 2080–2099 against the reference period (1986–2005). The abbreviations of all the investigated stations are described in Table 1.

5.3. Differences in Monthly Temperature and PET under Different RCP Scenarios

In this section, changes in the mean monthly PET and temperature between the three future time periods are presented for two emission scenarios in comparison to the historical period for all stations. The results for the first two future periods are discussed and illustrated in Supplementary Materials. In the RCP4.5 scenario, it can be observed that the mean monthly differences for the near future PET had two peaks: one during February and one in October. For each emission scenario, the PET changes for the near future were accompanied by changes in temperature, and the results show that for every 1 °C change in temperature influence, there was a two-fold increase in the PET. Similarly to the near-future time period, the mean PET and temperature differences for each month during the mid-future period (2046–2065) observed a PET increase during November, which reached a maximum in March and decreased until October, with a second peak appearing in July and August. In Darjeeling, the maximum PET changes occurred in July with constant temperature changes. The PET changes, particularly in Malda and Siliguri during the monsoon months, were not associated with an increase in temperature changes. This could be attributed to humidity. The maximum PET changes for each station under the RCP4.5 scenario vary between 3 and 4 °C and during the period from March to April. In the RCP8.5 scenario, the highest PET changes ranged between 4 and 5 °C during post-winter months. The mean monthly differences of PET and temperature for the far future (2080–2099) time period compared to the historical (1986–2005) time period for all stations are illustrated in Figure 5. It can be observed that the PET changes increased along with an increase in temperature from January while reaching a maximum during March and April. In the RCP4.5 scenario, for the period of January to April, the PET varied between 2.4 °C and 4.8 °C and was likely caused by a positive increment in temperature, which ranged between 2 °C and 3.4 °C. The mean monthly PET and temperature changes in the RCP8.5 scenario during the end of the twenty-first century followed a similar pattern when compared to the RCP4.5 scenario. However, the PET magnified two-fold under the RCP8.5 scenario in comparison to the RCP4.5 scenario. The largest PET changes occurred from January to April and varied between 5 and 9 °C, and the change was forced by temperature changes between 4.9 and 7.0 °C. The highest PET changes close to 9 °C were observed in Sriniketan, Asansol, Birbhum, Malda, Kolkata, Dum Dum, Kharagpur, Chinsurah, Krishnanagar, and Siliguri.

5.4. Importance of Data Quality in Estimating Human Bioclimate Conditions

To establish the importance of data quality, a correlation study has been conducted by using two different data sources, i.e., ERA-5 and the Indian Monsoon Data Assimilation and Analysis (IMDAA) reanalysis. IMDAA is a regional atmospheric reanalysis over the Indian subcontinent with a horizontal resolution of about 12 km [76]. The fifth-generation reanalysis popularly known as ERA-5 (spatial resolution ~31 km), released by ECMWF, is an upgraded version of Era-Interim (spatial resolution ~79 km) in terms of spatial resolution [77]. In this data quality test, we chose three stations, namely Alipore (Kolkata), Diamond Harbour, and Darjeeling. Kolkata is an urban station; Diamond Harbour lies close to the sea; Darjeeling is a high-altitude station. In order to calculate the correlation coefficient, we chose the daily observed station data, provided by the Indian Meteorological Department (IMD), for the period from 2020 to 2021 at 0830 h (IST) and 1430 h (IST). The descriptive statistics of air temperature, relative humidity, wind speed, and cloud cover and the computed PET for the mentioned period during mornings and afternoons are presented in Tables 3 and 4, respectively. The correlation coefficient value and confidence interval in brackets for each variable between ERA-5 and IMDAA against IMD are illustrated in Table 5. The highest agreement was observed for air temperature, followed by relative humidity, wind speed, and cloud cover. The correlation values in Table 4 strongly indicate that ERA-5 is better than IMDAA.

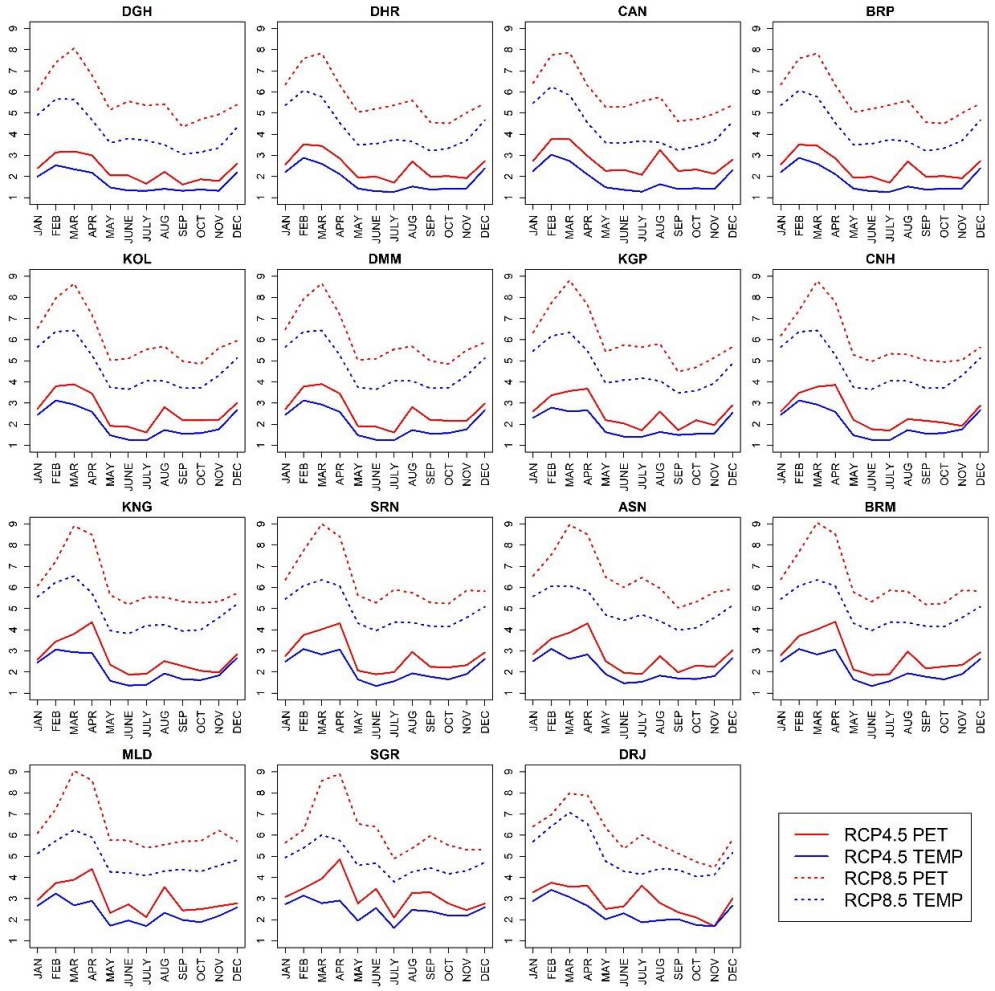

Figure 5. PET and temperature differences for each month under RCP4.5 and RCP8.5 from CORDEX during 2080–2099 relative to the reference period (1986–2005). The abbreviations of all investigated stations are described in Table 1.

Table 3. Comparison of the descriptive statistics for temperature, relative humidity, wind speed, and cloud cover from ERA-5, IMDAA, and IMD. PET has been calculated by RayMan using daily data from 2020 to 2021 at 0830 h (IST). Three stations, namely Alipore (Kolkata), Diamond Harbour, and Darjeeling, have been chosen for this comparative study.

	IMD	**0830 h**			**ERA5**	**0830 h**		**IMDAA**	**0830 h**	
Variables	**Station**	**Minimum**	**Maximum**	**Mean**	**Minimum**	**Maximum**	**Mean**	**Minimum**	**Maximum**	**Mean**
Temperature (°C)	Alipore (Kolkata)	14	33.4	25.9	14.1	34.2	25.9	13.6	35.3	25.9
	Diamond Harbour	14	34	25.8	14.3	34.5	26.2	15.1	33.9	26.6
	Darjeeling	2.4	30.2	13.3	7.3	27.7	18.6	8.4	28.4	19
Relative Humidity (%)	Alipore (Kolkata)	40	100	78.6	41	100	78.7	37.4	99.3	76.7
	Diamond Harbour	57	100	87	41.2	100	79.5	36.8	99.5	76.6
	Darjeeling	39	100	85.6	41.5	100	79.5	44.7	98.1	78.3

Table 3. *Cont.*

	IMD	0830 h			ERA5	0830 h		IMDAA	0830 h	
Variables	**Station**	**Minimum**	**Maximum**	**Mean**	**Minimum**	**Maximum**	**Mean**	**Minimum**	**Maximum**	**Mean**
Wind Speed (ms^{-1})	Alipore (Kolkata)	0	4.6	1.2	0.1	9.3	2.5	0.1	9.2	2.6
	Diamond Harbour	0	5.1	0.2	0.1	9.1	2.6	0.1	12.8	3.5
	Darjeeling	0	0.1	0.04	0	2.4	0.7	0.1	2.5	1
Cloud Cover (Octas)	Alipore (Kolkata)	0	8	3.8	0	8	1.6	0	7.9	0.8
	Diamond Harbour	0	8	3.8	0	8	1.8	0	7.8	0.7
	Darjeeling	0	8	4.2	0	8	2.9	0	8	1.5
PET (°C)	Alipore (Kolkata)	12.5	48.1	33.1	12.7	45	30	10.5	43.4	29.9
	Diamond Harbour	11.5	51.1	35.8	12.8	45.7	30.2	10.9	44.6	29.9
	Darjeeling	2.1	46.4	22.9	5.3	42.8	25.5	4	41.7	23.4

Table 4. Comparison of the descriptive statistics for temperature, relative humidity, wind speed, and cloud cover from ERA-5, IMDAA, and IMD. PET has been calculated by RayMan using daily data from 2020 to 2021 at 1430 h (IST). Three stations, namely Alipore (Kolkata), Diamond Harbour, and Darjeeling, have been chosen for this comparative study.

	IMD	1430 h			ERA5	1430 h		IMDAA	1430 h	
Variables	**Station**	**Minimum**	**Maximum**	**Mean**	**Minimum**	**Maximum**	**Mean**	**Minimum**	**Maximum**	**Mean**
Temperature (°C)	Alipore (Kolkata)	17.4	39.0	30.2	18.2	39.5	30.8	17.5	41.0	30.9
	Diamond Harbour	17.6	37.6	30.5	18.2	39.2	30.8	16.7	39.6	30.0
	Darjeeling	5.0	25.0	16.2	9.5	29.4	22.1	10.2	28.6	21.3
Relative Humidity (%)	Alipore (Kolkata)	19.0	99.0	60.8	16.8	95.9	60.5	11.8	93.8	54.2
	Diamond Harbour	28.0	100	71.5	13.9	99.5	61.4	16.2	90.8	59.3
	Darjeeling	35.0	100	77.1	29.0	10	73.1	28.3	99.4	72.9
Wind Speed (ms^{-1})	Alipore (Kolkata)	0.0	17.5	1.3	0.3	12.7	2.7	0.0	7.9	0.6
	Diamond Harbour	0.0	5.7	0.4	0.2	13.9	2.8	0.4	23.9	4.1
	Darjeeling	0.0	0.1	0.04	0.1	2.5	1.3	0.1	3.5	1.7
Cloud Cover (Octas)	Alipore (Kolkata)	0.0	8.0	4.2	0.0	8.0	1.4	0.0	7.9	0.6
	Diamond Harbour	0.0	8.0	3.6	0.0	8.0	1.4	0.0	7.7	0.5
	Darjeeling	0.0	8.0	5.8	0.0	8.0	3.2	0.0	8.0	1.2
PET (°C)	Alipore (Kolkata)	14.9	50.9	37.8	15.4	49.5	36.1	17.5	47.9	35.9
	Diamond Harbour	21.1	52.9	41.9	16.0	50.1	36.0	12.5	48.9	33.7
	Darjeeling	5.6	40.6	28.0	9.7	40.7	25.6	5.6	40.2	24.3

Table 5. Correlation coefficient values for air temperature, relative humidity, wind speed, cloud cover, and PET variables from ERA-5 and IMDAA against observed data measured by IMD. The period of analysis is over daily data from January 2020 to December 2021 at 0830 h (IST) and 1430 h (IST).

Variables	Station at 0830 h	ERA5	IMDAA	Station at 1430 h	ERA5	IMDAA
Temperature (°C)	Alipore (Kolkata)	0.98 (0.982–0.987)	0.97 (0.964–0.973)	Alipore (Kolkata)	0.95 (0.937–0.953)	0.91 (0.897–0.923)
	Diamond Harbour	0.99 (0.983–0.987)	0.96 (0.958–0.969)	Diamond Harbour	0.92 (0.908–0.931)	0.88 (0.856–0.892)
	Darjeeling	0.97 (0.963–0.973)	0.90 (0.899–0.927)	Darjeeling	0.83 (0.804–0.851)	0.82 (0.787–0.839)
Relative Humidity (%)	Alipore (Kolkata)	0.74 (0.701–0.770)	0.66 (0.614–0.700)	Alipore (Kolkata)	0.90 (0.887–0.915)	0.86 (0.843–0.881)
	Diamond Harbour	0.59 (0.544–0.641)	0.50 (0.445–0.557)	Diamond Harbour	0.84 (0.813–0.859)	0.82 (0.790–0.840)
	Darjeeling	0.40 (0.331–0.456)	0.43 (0.368–0.490)	Darjeeling	0.68 (0.641–0.722)	0.57 (0.520–0.623)
Wind Speed (ms^{-1})	Alipore (Kolkata)	0.61 (0.559–0.654)	0.56 (0.506–0.611)	Alipore (Kolkata)	0.49 (0.427–0.542)	0.41 (0.347–0.473)
	Diamond Harbour	0.45 (0.384–0.504)	0.37 (0.308–0.438)	Diamond Harbour	0.37 (0.301–0.431)	0.37 (0.304–0.435)
	Darjeeling	0.13 (0.056–0.202)	−0.08 (−0.156–−0.008)	Darjeeling	−0.05 (−0.126–0.025)	−0.269 (−0.339–−0.196)
Cloud Cover (Octas)	Alipore (Kolkata)	0.50 (0.440–0.554)	0.26 (0.183–0.326)	Alipore (Kolkata)	0.49 (0.427–0.542)	0.18 (0.108–0.254)
	Diamond Harbour	0.49 (0.433–0.546	0.30 (0.227–0.364)	Diamond Harbour	0.54 (0.488–0.594)	0.24 (0.172–0.314)
	Darjeeling	0.57 (0.522–0.622)	0.18 (0.106–0.251)	Darjeeling	0.27 (0.200–0.339)	0.098 (0.021–0.173)
PET (°C)	Alipore (Kolkata)	0.84 (0.817–0.862)	0.81 (0.780–0.834)	Alipore (Kolkata)	0.86 (0.834–0.874)	0.80 (0.769–0.824)
	Diamond Harbour	0.76 (0.721–0.786)	0.70 (0.662–0.739)	Diamond Harbour	0.69 (0.648–0.727)	0.60 (0.546–0.644)
	Darjeeling	0.57 (0.516–0.617)	0.51 (0.458–0.567)	Darjeeling	0.58 (0.529–0.630)	0.52 (0.461–0.573)

6. Discussion

Human thermal conditions in 15 stations across WB were computed using a time series of air temperature, relative humidity, wind speed, and cloud cover by using the RayMan model. This was performed for the past period and three future time periods. The monthly PET varied from very cool to hot conditions. Heat stress conditions comprised slightly warm, warm, and hot classes, which began in April, with all stations exhibiting more than 80% share except for Darjeeling. The present results evolved from intra-annual PET class variations across WB. The results obtained in this study concurred with the results of recent studies conducted in eastern India using different thermal indices, which identified December and January as the most comfortable months. On the other hand, March and April were identified as the most stressful months in terms of human thermal comfort [20,55]. The frequency spectrum of thermal stress categories was computed from the 15 sites across WB, and the data obtained suggested a spatial variability of PET in this part of the country. Simultaneously, this study targeted 15 sites across WB in order to delineate the future human bioclimate conditions. Furthermore, the projected PET changes

influenced by temperature changes in each month were investigated to discern the influence of temperature on PET. It was observed that under a high-emission scenario during the period from 2080 to 2099, stations close to the Bay of Bengal such as Digha, Diamond Harbour, Canning, and Baruipur exhibited the largest positive warm stress changes. A similar pattern of heat stress conditions was also reported in previous studies by Rao, Kumar [58] and Jaswal, Padmakumari [20]. The latter study recognized the Southeast coastal regions as being the most vulnerable in summer months and the northwest coastal regions and Indo-Gangetic plains as being vulnerable during monsoons [20]. Recent studies have also projected heat stress over India under different emission scenarios and have reported that the eastern coastal region would suffer from more heat stress days in comparison to western coastal regions [50,51,58].

Extreme thermal conditions designated as hot conditions in PET exhibited the highest positive changes in Sriniketan, Asonsol, Birbhum, Malda, Kolkata, Dum Dum, Kharagpur, and Siliguri. This observation of thermal discomfort could be attributed to the urban sprawl in these sites. Past studies have noted that an unchecked spread in human settlements can result in an increase in population share, which further increases the surface heat capacity and finally adds to the mean surface temperature [56,78,79]. Studies have also noted that the absorption and re-emission of particles by anthropogenic activities activated the growth of cloud condensation nuclei, thereby leading to increased air humidity [80,81]. One study also observed that reduced wind speeds due to dense and high-rise settlements drastically depreciated human thermal conditions [82]. The mean values of the driving variables along with their descriptive statistics for the past period and future years are highlighted in Tables S1–S3 in the Supplementary Materials section. Future intense heat episodes that critically influence human health are projected to occur often and more acutely in the regions selected for this study. As a result, there is a need to extend the scope of the current study by accounting for the consequences of short-term acclimatization, the impact on different age groups, the living status of an individual, indoor environment, and building designs and the materials they are constructed with. These criteria will assist in future assessments and play a vital role in implementing improvement measures with respect to reducing thermal stress. To inhibit the detrimental aspects of thermal stress, the presence of an accurate and timely heat-health warning system is crucial. At present, the majority of WB is currently experiencing a rapid urbanization process. Therefore, small-scale environmental planning at the town level should be upgraded to reduce the significant impacts of extreme human bioclimate conditions in WB. Past studies have suggested the potential steps of using cool roofing, green terraces, paving materials, tree planting, and vegetable cultivation, ensuring more water bodies in open spaces, etc., as means of reducing negative impacts [80,83,84]. The outcome of this present study highlights the utility of PET signatures for the bioclimatic forecast, which consequently could serve as an input for urban planners, public health policy makers, the tourism industry, and outdoor event organizers. A past study noted that in order to focus on the comprehensive spatial distribution of the human thermal environment, a bioclimatic mapping comprising urban and suburban micrometeorological observations should be given the highest priority [85]. Building upon this, two other studies observed that this would help in distinguishing between acceptable or less acceptable human thermal conditions, particularly in human settlements [52,55].

7. Conclusions

The present study investigated the thermal bioclimate conditions for fifteen stations across WB during the period (1986–2005) and for three future time periods. The conflict in separating the most unpleasant towns in WB by existing climate models might be due to the coarse grid in the existing model. For example, the time series of the atmospheric variables for neighboring stations are homologous and do not separate human bio-environment conditions. This could be attributed to the fact that these stations lie in the same grid box. It can be stated that with a high-quality data input, the model was capable of computing realistic human bioclimate conditions. Therefore, future research should consider data

sources comprising climate projections using improved resolutions over the proposed study region. Furthermore, the hourly data of each day were deemed essential for expressing the diurnal variation in health-related thermal conditions. As a result, additional bioclimate indices that are based on human heat budget models similar to PET and SET should be employed by concerned departments for providing trustworthy statistics and recommending responsible measures. Future research should also emphasize upgrading thermal comfort indices such as mPET and should be adapted by local administrators to take necessary measurements for citizens.

Supplementary Materials: The following supporting information can be downloaded at https://www.mdpi.com/article/10.3390/atmos14030505/s1. Figure S1: Intra-annual frequency diagram of different PET classes over the investigated stations extracted from the CORDEX under RCP4.5 condition during 2016–2035, Figure S2: Intra-annual frequency diagram of different PET classes over the investigated stations extracted from the CORDEX under RCP4.5 condition during 2046–2065, Figure S3: Intra-annual frequency diagram of different PET classes over the investigated stations extracted from the CORDEX under RCP4.5 condition during 2080–2099, Figure S4 to S6: Intra-annual frequency diagram of different PET classes over the investigated stations extracted from the CORDEX under the RCP8.5 condition during (2016–2035), (2046–2065), and (2080–2099). Figure S7 to S8: Mean monthly differences of PET and temperature for 15 considered stations in WB under RCP4.5 and RCP8.5 from CORDEX with respect to the reference period during (2016–2035) and (2046–2065). Table S1 to S3: Descriptive statistics for all variables for the period from 1986 to 2005 and the future periods of (2016–2035), (2046–2065), and (2080–2099) under both emissions scenarios.

Author Contributions: S.B., as the corresponding author, pursued the idea and analyzed all datasets, results, and prepared the draft; I.K. was involved and helped in interpreting and improving both the results and the manuscript. All authors have read and agreed to the published version of the manuscript.

Funding: This research received no funding.

Institutional Review Board Statement: Not applicable.

Informed Consent Statement: Not applicable.

Data Availability Statement: Meteorological datasets used in this study can all be obtained from publicly accessible archives. The codes and visualizations required for the study were made in R software. The data and code are available from the corresponding author upon reasonable request.

Acknowledgments: The authors would like to thank the Indian Meteorological Department, Kolkata, for the station data. Climate model data are provided by CORDEX-South Asia.

Conflicts of Interest: The author declares no conflict of interest.

References

1. Flato, G.; Marotzke, J.; Abiodun, B.; Braconnot, P.; Chou, S.C.; Collins, W. Evaluation of climate models. In *Climate Change 2013: The Physical Science Basis. Contribution of Working Group I to the Fifth Assessment Report of the Intergovernmental Panel on Climate Change*; Cambridge University Press: Cambridge, UK; New York, NY, USA, 2014; pp. 741–866.
2. van Oldenborgh, G.J.; Collins, M.; Arblaster, J.; Christensen, J.H.; Marotzke, J.; Power, S.B.; Rummukainen, M.; Zhou, T. Annex I: Atlas of Global and Regional Climate Projections. In *Climate Change 2013: The Physical Science Basis. Contribution of Working Group I to the Fifth Assessment Report of the Intergovernmental Panel on Climate Change*; Stocker, T.F., Qin, D., Plattner, G.-K., Tignor, M., Allen, S., Boschung, J., Nauels, A., Xia, Y., Bex, V., Midgley, P., Eds.; Cambridge University Press: Cambridge, UK; New York, NY, USA, 2013.
3. Stocker, T.F.; Qin, D.; Plattner, G.-K.; Tignor, M.; Allen, S.; Boschung, J.; Nauels, A.; Xia, Y.; Bex, V.; Midgley, P. *Climate Change 2013: The Physical Science Basis. Contribution of Working Group I to the Fifth Assessment Report of the Intergovernmental Panel on Climate Change*; Cambridge University Press: Cambridge, UK; New York, NY, USA, 2013; p. 1535.
4. IPCC. *The Physical Science Basis: Contribution of Working Group I to the Fourth Assessment Report of the Intergovernmental Panel on Climate Change*; Cambridge University Press: Cambridge, UK; New York, NY, USA, 2007; Volume 996.
5. Stocker, T.F.; Qin, D.; Plattner, G.-K.; Alexander, L.V.; Allen, S.K.; Bindoff, N.L.; Bréon, F.-M.; Church, J.A.; Cubasch, U.; Emori, S. Technical summary. In *Climate Change 2013: The Physical Science Basis. Contribution of Working Group I to the Fifth Assessment Report of the Intergovernmental Panel on Climate Change*; Cambridge University Press: Cambridge, UK; New York, NY, USA, 2013; pp. 33–115.

6. Trenberth, K.E.; Jones, P.D.; Ambenje, P.; Bojariu, R.; Easterling, D.; Tank, A.K.; Parker, D.; Rahimzadeh, F.; Renwick, J.A.; Rusticucci, M. Observations: Surface and atmospheric climate change. In *Climate Change 2007: The Physical Science Basis. Contribution of Working Group 1 to the 4th Assessment Report of the Intergovernmental Panel on Climate Change*; Cambridge University Press: Cambridge, UK; New York, NY, USA, 2007.
7. Meehl, G.A.; Tebaldi, C. More Intense, More Frequent, and Longer Lasting Heat Waves in the 21st Century. *Science* **2004**, *305*, 994–997. [CrossRef]
8. Coumou, D.; Rahmstorf, S. A decade of weather extremes. *Nat. Clim. Chang.* **2012**, *2*, 491–496. [CrossRef]
9. Perkins, S.E.; Alexander, L.V.; Nairn, J.R. Increasing frequency, intensity and duration of observed global heatwaves and warm spells. *Geophys. Res. Lett.* **2012**, *39*, 10. [CrossRef]
10. García-Herrera, R.; Díaz, J.; Trigo, R.M.; Luterbacher, J.; Fischer, E.M. A review of the European summer heat wave of 2003. *Crit. Rev. Environ. Sci. Technol.* **2010**, *40*, 267–306. [CrossRef]
11. Diffenbaugh, N.S.; Ashfaq, M. Intensification of hot extremes in the United States. *Geophys. Res. Lett.* **2010**, *37*, 1–14. [CrossRef]
12. Ding, T.; Qian, W.; Yan, Z. Changes in hot days and heat waves in China during 1961–2007. *Int. J. Clim.* **2009**, *30*, 1452–1462. [CrossRef]
13. Tank, A.M.G.K.; Peterson, T.C.; Quadir, D.A.; Dorji, S.; Zou, X.; Tang, H.; Santhosh, K.; Joshi, U.R.; Jaswal, A.K.; Kolli, R.K.; et al. Changes in daily temperature and precipitation extremes in central and south Asia. *J. Geophys. Res. Atmos.* **2006**, *111*, D16105. [CrossRef]
14. Kothawale, D.R.; Kumar, K.R. On the recent changes in surface temperature trends over India. *Geophys. Res. Lett.* **2005**, *32*, 18714. [CrossRef]
15. Mukherjee, S.; Mishra, V. A sixfold rise in concurrent day and night-time heatwaves in India under 2 °C warming. *Sci. Rep.* **2018**, *8*, 16922. [CrossRef] [PubMed]
16. Rai, A.; Joshi, M.K.; Pandey, A.C. Variations in diurnal temperature range over India: Under global warming scenario. *J. Geophys. Res. Atmos.* **2012**, *117*, D02114. [CrossRef]
17. Vinnarasi, R.; Dhanya, C.T.; Chakravorty, A.; AghaKouchak, A. Unravelling Diurnal Asymmetry of Surface Temperature in Different Climate Zones. *Sci. Rep.* **2017**, *7*, 7350. [CrossRef]
18. Pai, D.; Nair, S.; Ramanathan, A. Long term climatology and trends of heat waves over India during the recent 50 years (1961–2010). *Mausam* **2013**, *64*, 585–604. [CrossRef]
19. Rohini, P.; Rajeevan, M.; Srivastava, A.K. On the Variability and Increasing Trends of Heat Waves over India. *Sci. Rep.* **2016**, *6*, 26153. [CrossRef]
20. Jaswal, A.; Padmakumari, B.; Kumar, N.; Kore, P. Increasing Trend in Temperature and Moisture Induced Heat Index and Its Effect on Human Health in Climate Change Scenario over the Indian Sub-continent. *J. Clim. Chang.* **2017**, *3*, 11–25. [CrossRef]
21. De, U.; Dube, R.K.; Rao, G.P. Extreme weather events over India in the last 100 years. *J. Ind. Geophys. Union* **2005**, *9*, 173–187.
22. Das, B.; Chakraborty, R. Climate Change Scenario of West Bengal, India: A Geo-Environmental Assessment. *Indian Cartogr.* **2016**, *36*, 425–441.
23. Jha, V.C. Indian Cartographer. 2016. Available online: https://www.academia.edu/36558530/Indian_Cartographer_Vol_36_Part_I_2016_ISSN_0927_8392_pdf (accessed on 19 February 2023).
24. Government of West Bengal. *West Bengal State Action Plan on Climate Change (WBAPCC, 2012) Repor*; Government of West Bengal, Government of India: Howrah, India, 2012. Available online: http://www.nicra-icar.in/nicrarevised/images/State%20Action%20Plan/West-Bengal-SAPCC.pdf (accessed on 19 February 2023).
25. Azhar, G.S.; Mavalankar, D.; Nori-Sarma, A.; Rajiva, A.; Dutta, P.; Jaiswal, A.; Sheffield, P.; Knowlton, K.; Hess, J.J.; Ahmedabad HeatClimate Study Group. Heat-Related Mortality in India: Excess All-Cause Mortality Associated with the 2010 Ahmedabad Heat Wave. *PLoS ONE* **2014**, *9*, e91831. [CrossRef] [PubMed]
26. Bal, S.; Sodoudi, S. Modeling and prediction of dengue occurrences in Kolkata, India, based on climate factors. *Int. J. Biometeorol.* **2020**, *64*, 1379–1391. [CrossRef]
27. Landsberg, H.E. *The Assessment of Human Bioclimate*; World Meteorological Organization (WMO): Geneva, Switzerland, 1972.
28. Gagge, A.P.; Fobelets, A.; Berglund, L. A standard predictive Index of human reponse to thermal enviroment. *Trans.Am. Soc. Heat. Refrig. Air-Cond. Eng.* **1986**, *92*, 709–731.
29. Staiger, H.; Laschewski, G.; Grätz, A. The perceived temperature–a versatile index for the assessment of the human thermal environment. Part A: Scientific basics. *Int. J. Biometeorol.* **2012**, *56*, 165–176. [CrossRef] [PubMed]
30. Höppe, P. The physiological equivalent temperature–A universal index for the biometeorological assessment of the thermal environment. *Int. J. Biometeorol.* **1999**, *43*, 71–75. [CrossRef]
31. Blazejczyk, K.; Epstein, Y.; Jendritzky, G.; Staiger, H.; Tinz, B. Comparison of UTCI to selected thermal indices. *Int. J. Biometeorol.* **2012**, *56*, 515–535. [CrossRef]
32. Havenith, G.; Fiala, D.; Błazejczyk, K.; Richards, M.; Bröde, P.; Holmér, I.; Rintamaki, H.; Benshabat, Y.; Jendritzky, G. The UTCI-clothing model. *Int. J. Biometeorol.* **2012**, *56*, 461–470. [CrossRef] [PubMed]
33. Jendritzky, G.; de Dear, R.; Havenith, G. UTCI—Why another thermal index? *Int. J. Biometeorol.* **2012**, *56*, 421–428. [CrossRef] [PubMed]
34. Staiger, H.; Laschewski, G.; Matzarakis, A. Selection of Appropriate Thermal Indices for Applications in Human Biometeorological Studies. *Atmosphere* **2019**, *10*, 18. [CrossRef]

35. Fiala, D.; Havenith, G.; Bröde, P.; Kampmann, B.; Jendritzky, G. UTCI-Fiala multi-node model of human heat transfer and temperature regulation. *Int. J. Biometeorol.* **2012**, *56*, 429–441. [CrossRef]
36. Krüger, E.; Rossi, F.; Drach, P. Calibration of the physiological equivalent temperature index for three different climatic regions. *Int. J. Biometeorol.* **2017**, *61*, 1323–1336. [CrossRef]
37. Galindo, T.; Hermida, M.A. Effects of thermophysiological and non-thermal factors on outdoor thermal perceptions: The Tomebamba Riverbanks case. *Build. Environ.* **2018**, *138*, 235–249. [CrossRef]
38. Krüger, E.L.; Costa, T. Interferences of urban form on human thermal perception. *Sci. Total. Environ.* **2019**, *653*, 1067–1076. [CrossRef]
39. Amindeldar, S.; Heidari, S.; Khalili, M. The effect of personal and microclimatic variables on outdoor thermal comfort: A field study in Tehran in cold season. *Sustain. Cities Soc.* **2017**, *32*, 153–159. [CrossRef]
40. Ndetto, E.L.; Matzarakis, A. Assessment of human thermal perception in the hot-humid climate of Dar es Salaam, Tanzania. *Int. J. Biometeorol.* **2017**, *61*, 69–85. [CrossRef]
41. Matzarakis, A.; Mayer, H.; Iziomon, M. Applications of a universal thermal index: Physiological equivalent temperature. *Int. J. Biometeorol.* **1999**, *43*, 76–84. [CrossRef]
42. Mayer, H.; Höppe, P. Thermal comfort of man in different urban environments. *Theor. Appl. Climatol.* **1987**, *38*, 43–49. [CrossRef]
43. Jendritzky, G.; Bucher, K.; Laschewski, G.; Walther, H. Atmospheric heat exchange of the human being, bioclimate assessments, mortality and thermal stress. *Int. J. Circumpolar Health* **2000**, *59*, 222. [PubMed]
44. Gonzalez, R.; Nishi, Y.; Gagge, A. Experimental evaluation of standard effective temperature a new biometeorological index of man's thermal discomfort. *Int. J. Biometeorol.* **1974**, *18*, 1–15. [CrossRef]
45. Matzarakis, A. Weather- and climate-related information for tourism. *Tour. Hosp. Plan. Dev.* **2006**, *3*, 99–115. [CrossRef]
46. Rodríguez-Algeciras, J.; Algeciras, J.A.R.; Chaos-Yeras, M.; Matzarakis, A. Tourism-related climate information for adjusted and responsible planning in the tourism industry in Barcelona, Spain. *Theor. Appl. Clim.* **2020**, *142*, 1003–1014. [CrossRef]
47. Lin, T.-P.; Matzarakis, A. Tourism climate information based on human thermal perception in Taiwan and Eastern China. *Tour. Manag.* **2011**, *32*, 492–500. [CrossRef]
48. Chen, Y.-C.; Matzarakis, A. Modified physiologically equivalent temperature—Basics and applications for western European climate. *Theor. Appl. Clim.* **2018**, *132*, 1275–1289. [CrossRef]
49. IPCC. Future Global Climate: Scenario-Based Projections and Near-Term Information. 2021. Available online: https://www.ipcc.ch/report/ar6/wg1/downloads/report/IPCC_AR6_WGI_FOD_Chapter04.pdf (accessed on 19 February 2023).
50. Zachariah, M.; Arulalan, T.; AchutaRao, K.; Saeed, F.; Jha, R.; Dhasmana, M.; Mondal, A.; Bonnet, R.; Vautard, R.; Philip, S. Climate Change Made Devastating Early Heat in India and Pakistan 30 Times More Likely. *World Weather Attrib.* 2022. Available online: https://www.worldweatherattribution.org/wp-content/uploads/India_Pak-Heatwave-scientific-report.pdf (accessed on 19 February 2023).
51. Raymond, C.; Matthews, T.; Horton, R.M. The emergence of heat and humidity too severe for human tolerance. *Sci. Adv.* **2020**, *6*, eaaw1838. [CrossRef]
52. Banerjee, S.; Middel, A.; Chattopadhyay, S. Outdoor thermal comfort in various microentrepreneurial settings in hot humid tropical Kolkata: Human biometeorological assessment of objective and subjective parameters. *Sci. Total. Environ.* **2020**, *721*, 137741. [CrossRef] [PubMed]
53. Das, M.; Das, A.; Mandal, S. Outdoor thermal comfort in different settings of a tropical planning region of Eastern India by adopting LCZs approach: A case study on Sriniketan-Santiniketan Planning Area (SSPA). *Sustain. Cities Soc.* **2020**, *63*, 102433. [CrossRef]
54. Sen, J.; Nag, P.K. Human susceptibility to outdoor hot environment. *Sci. Total. Environ.* **2018**, *649*, 866–875. [CrossRef] [PubMed]
55. Ziaul, S.; Pal, S. Assessing outdoor thermal comfort of English Bazar Municipality and its surrounding, West Bengal, India. *Adv. Space Res.* **2019**, *64*, 567–580. [CrossRef]
56. De, B.; Mukherjee, M. Optimisation of canyon orientation and aspect ratio in warm-humid climate: Case of Rajarhat Newtown, India. *Urban Clim.* **2018**, *24*, 887–920. [CrossRef]
57. Bhattacharya, R.; Biswas, G.; Guha, R.; Pal, S.; Dey, S. On the variation of summer thermal stress over Kolkata from 1995 to 2009. *VAYU MANDAL* **2010**, *35–36*, 16–21.
58. Rao, K.K.; Kumar, T.V.L.; Kulkarni, A.; Ho, C.-H.; Mahendranath, B.; Desamsetti, S.; Patwardhan, S.; Dandi, A.R.; Barbosa, H.; Sabade, S. Projections of heat stress and associated work performance over India in response to global warming. *Sci. Rep.* **2020**, *10*, 16675. [CrossRef]
59. IMD. Climate of West Bengal. 2008. Available online: https://imdpune.gov.in/library/public/Climate%20of%20WestBengal.pdf (accessed on 19 February 2023).
60. Bal, S.; Matzarakis, A. Temporal analysis of thermal bioclimate conditions between Kolkata (India) and its three neighbouring suburban sites. *Theor. Appl. Clim.* **2022**, *148*, 1545–1562. [CrossRef]
61. Sanjay, J.; Krishnan, R.; Shrestha, A.B.; Rajbhandari, R.; Ren, G.-Y. Downscaled climate change projections for the Hindu Kush Himalayan region using CORDEX South Asia regional climate models. *Adv. Clim. Chang. Res.* **2017**, *8*, 185–198. [CrossRef]
62. Chi, X.; Cubasch, U.; Sodoudi, S. Assessment of human bio-meteorological environment over the Tibetan Plateau region based on CORDEX climate model projections. *Theor. Appl. Clim.* **2019**, *137*, 893–907. [CrossRef]

63. Lokys, H.L.; Junk, J.; Krein, A. Future Changes in Human-Biometeorological Index Classes in Three Regions of Luxembourg, Western-Central Europe. *Adv. Meteorol.* **2015**, *2015*, 323856. [CrossRef]
64. Matzarakis, A.; Rutz, F.; Mayer, H. Modelling radiation fluxes in simple and complex environments—Application of the RayMan model. *Int. J. Biometeorol.* **2007**, *51*, 323–334. [CrossRef]
65. Matzarakis, A.; Rutz, F.; Mayer, H. Modelling radiation fluxes in simple and complex environments: Basics of the RayMan model. *Int. J. Biometeorol.* **2010**, *54*, 131–139. [CrossRef]
66. VDI. *Part I: Environmental Meteorology, Methods for the Human Biometeorological Evaluation of Climate and Air Quality for the Urban and Regional Planning at Regional Level*; Part I: Climate; Beuth: Berlin, Germany, 1998; Volume 3787.
67. Ndetto, E.L.; Matzarakis, A. Basic analysis of climate and urban bioclimate of Dar es Salaam, Tanzania. *Theor. Appl. Clim.* **2013**, *114*, 213–226. [CrossRef]
68. Pecelj, M.; Matzarakis, A.; Vujadinović, M.; Radovanović, M.; Vagić, N.; Đurić, D.; Cvetkovic, M. Temporal Analysis of Urban-Suburban PET, mPET and UTCI Indices in Belgrade (Serbia). *Atmosphere* **2021**, *12*, 916. [CrossRef]
69. Elnabawi, M.H.; Hamza, N.; Dudek, S. Thermal perception of outdoor urban spaces in the hot arid region of Cairo, Egypt. *Sustain. Cities Soc.* **2016**, *22*, 136–145. [CrossRef]
70. Tsitoura, M.; Tsoutsos, T.; Daras, T. Evaluation of comfort conditions in urban open spaces. *Application in the island of Crete. Energy Convers. Manag.* **2014**, *86*, 250–258. [CrossRef]
71. Lin, T.-P.; Matzarakis, A. Tourism climate and thermal comfort in Sun Moon Lake, Taiwan. *Int. J. Biometeorol.* **2007**, *52*, 281–290. [CrossRef]
72. Chatterjee, S.; Khan, A.; Dinda, A.; Mithun, S.; Khatun, R.; Akbari, H.; Kusaka, H.; Mitra, C.; Bhatti, S.S.; Van Doan, Q.; et al. Simulating micro-scale thermal interactions in different building environments for mitigating urban heat islands. *Sci. Total. Environ.* **2018**, *663*, 610–631. [CrossRef] [PubMed]
73. Chatterjee, S.; Gupta, K. Exploring the spatial pattern of urban heat island formation in relation to land transformation: A study on a mining industrial region of West Bengal, India. *Remote Sens. Appl. Soc. Environ.* **2021**, *23*, 100581. [CrossRef]
74. Ghosh, S.; Das, A. Modelling urban cooling island impact of green space and water bodies on surface urban heat island in a continuously developing urban area. *Model. Earth Syst. Environ.* **2018**, *4*, 501–515. [CrossRef]
75. Dhar, R.B.; Chakraborty, S.; Chattopadhyay, R.; Sikdar, P.K. Impact of Land-Use/Land-Cover Change on Land Surface Temperature Using Satellite Data: A Case Study of Rajarhat Block, North 24-Parganas District, West Bengal. *J. Indian Soc. Remote Sens.* **2019**, *47*, 331–348. [CrossRef]
76. Halder, B.; Bandyopadhyay, J.; Banik, P. Monitoring the effect of urban development on urban heat island based on remote sensing and geo-spatial approach in Kolkata and adjacent areas, India. *Sustain. Cities Soc.* **2021**, *74*, 103186. [CrossRef]
77. Khan, A.; Chatterjee, S. Numerical simulation of urban heat island intensity under urban–suburban surface and reference site in Kolkata, India. *Model. Earth Syst. Environ.* **2016**, *2*, 71. [CrossRef]
78. Mukhopadhyay, B.; Weitz, C.A.; Das, K. Indoor heat conditions measured in urban slum and rural village housing in West Bengal, India. *Build. Environ.* **2021**, *191*, 107567. [CrossRef]
79. Oke, T.R. *Boundary Layer Climates*; Routledge: London, UK, 2002.
80. Rani, S.I.; Arulalan, T.; George, J.P.; Rajagopal, E.N.; Renshaw, R.; Maycock, A.; Barker, D.M.; Rajeevan, M. IMDAA: High Resolution Satellite-era Reanalysis for the Indian Monsoon Region. *J. Clim.* **2021**, *34*, 5109–5133. [CrossRef]
81. Hersbach, H.; Bell, B.; Berrisford, P.; Hirahara, S.; Horányi, A.; Muñoz-Sabater, J.; Nicolas, J.; Peubey, C.; Radu, R.; Schepers, D. The ERA5 global reanalysis. *Q. J. R. Meteorol. Soc.* **2020**, *146*, 1999–2049. [CrossRef]
82. Matzarakis, A.; Laschewski, G.; Muthers, S. The Heat Health Warning System in Germany—Application and Warnings for 2005 to 2019. *Atmosphere* **2020**, *11*, 170. [CrossRef]
83. Krüger, E.; Drach, P.; Emmanuel, R.; Corbella, O. Urban heat island and differences in outdoor comfort levels in Glasgow, UK. *Theor. Appl. Clim.* **2013**, *112*, 127–141. [CrossRef]
84. Potchter, O.; Cohen, P.; Lin, T.-P.; Matzarakis, A. Outdoor human thermal perception in various climates: A comprehensive review of approaches, methods and quantification. *Sci. Total Environ.* **2018**, *631*, 390–406. [CrossRef]
85. Sharmin, T.; Steemers, K.; Humphreys, M. Outdoor thermal comfort and summer PET range: A field study in tropical city Dhaka. *Energy Build.* **2019**, *198*, 149–159. [CrossRef]